Review

Author for correspondence:
Uel J. McMahan
e-mail: grantser@tamu.edu

The structure and function of 'active zone material' at synapses

Joseph A. Szule, Jae Hoon Jung and Uel J. McMahan

Department of Biology, Texas A&M University, College Station, TX 77845, USA

The docking of synaptic vesicles on the presynaptic membrane and their priming for fusion with it to mediate synaptic transmission of nerve impulses typically occur at structurally specialized regions on the membrane called active zones. Stable components of active zones include aggregates of macromolecules, 'active zone material' (AZM), attached to the presynaptic membrane, and aggregates of Ca^{2+}-channels in the membrane, through which Ca^{2+} enters the cytosol to trigger impulse-evoked vesicle fusion with the presynaptic membrane by interacting with Ca^{2+}-sensors on the vesicles. This laboratory has used electron tomography to study, at macromolecular spatial resolution, the structure and function of AZM at the simply arranged active zones of axon terminals at frog neuromuscular junctions. The results support the conclusion that AZM directs the docking and priming of synaptic vesicles and essential positioning of Ca^{2+}-channels relative to the vesicles' Ca^{2+}-sensors. Here we review the findings and comment on their applicability to understanding mechanisms of docking, priming and Ca^{2+}-triggering at other synapses, where the arrangement of active zone components differs.

1. Introduction

Formation of a shared fusion pore between the membrane of a synaptic vesicle and the presynaptic plasma membrane enables discharge of neurotransmitter from the synaptic vesicle lumen into the synaptic cleft to mediate synaptic impulse transmission. The formation of the fusion pore is preceded by a succession of events that begins prior to impulse activity. Initially, the synaptic vesicle is directed to a specialized active zone on the presynaptic membrane, where the vesicle membrane is held in contact with, i.e. 'docks' on, the presynaptic membrane. The docked synaptic vesicle is then 'primed', bringing the vesicle membrane and presynaptic membrane at their contact site towards fusion threshold. Arrival of the impulse increases the conductance of Ca^{2+} through voltage gated Ca^{2+}-channels clustered in the presynaptic membrane at the active zone, raising the local concentration of Ca^{2+} in the cytosol. Binding of Ca^{2+} to Ca^{2+}-sensors of the vesicle membrane triggers fusion/merging of the vesicle membrane and presynaptic membrane at their contact site, which then spontaneously leads to the formation of the fusion pore [1]. Biochemistry and electrophysiology have provided much information about the proteins and biophysical mechanisms regulating each of these events [2–4].

In addition to docked synaptic vesicles and Ca^{2+}-channels, active zones include aggregates of macromolecules bound to the cytosolic surface of the presynaptic membrane. The size, shape and number of such aggregates at an active zone as well as the gross arrangement of docked synaptic vesicles relative to them can vary from one synaptic type to another within an animal species and for the same synaptic type between species. Some are named according to a distinctive structural feature, such as ribbons [5,6], or T-bars [7–9], but all are thought to have shared functions and can generally be referred to as active zone material (AZM). AZM is seen in greatest detail by electron microscopy in sections cut from fixed, plastic embedded tissue, where it is stained with heavy metals. It was discovered approximately 60 years ago using 2D transmission electron microscopy [10–12]. Based on its association with synaptic vesicles, it was suggested relatively soon thereafter that, among other possibilities, AZM directs synaptic vesicles towards the presynaptic membrane and holds them in readiness

for the arrival of a nerve impulse (e.g. [5,13]). These hypotheses were strengthened by later observations that synaptic vesicle fusion with the presynaptic membrane occurs just alongside AZM [14,15]. This laboratory's more recent adaptation of electron tomography for studying the structural relationships of cytosolic macromolecules in individual tissue sections [16–18] has made it possible to test and extend these hypotheses [17,19–21].

Macromolecules composing AZM are much thinner than the thinnest tissue section that can be cut (approx. 30 nm), and, for much of the AZM, they are densely packed. Thus, it is difficult to distinguish individual AZM macromolecules and examine their associations in an image from a tissue section obtained by conventional 2D electron microscopy, because the image lacks depth axis spatial information. Electron tomography provides a 3D reconstruction of a section by using a series of 2D electron microscopy projections collected at different tilt angles to obtain volumetric data [22]. Relationships of structures within a reconstructed section can then be examined either in serial virtual slices made through the reconstructed volume, each of which can be as much as 100–200 times thinner than a 30 nm thick tissue section, or in 3D surface models generated by segmenting structures of interest from the reconstructed volume [18]. This laboratory has used electron tomography to study, at 2–3 nm 3D spatial resolution, the relationships of AZM macromolecules to each other, to synaptic vesicles and to the presynaptic membrane at the simply arranged active zones of axon terminals at frog neuromuscular junctions fixed at rest or during synaptic activity. Altogether the findings indicate that the AZM at frog neuromuscular junctions is a multifunctional organelle that regulates the docking, priming and Ca^{2+}-triggering that leads to synaptic vesicle fusion with the presynaptic membrane after the arrival of a nerve impulse.

2. Material and methods

The studies were done on frog striated muscles (cutaneous pectoris). In most cases, the muscles were fixed with buffered glutaraldehyde and stained with buffered osmium tetroxide at room temperature. The osmolarity of each solution was the same as that of frog Ringer's solution. In some cases, the muscles were fixed with glutaraldehyde or by rapid freezing and then stained with osmium tetroxide and uranyl acetate by freeze-substitution [23–25] to test and control for any potential room temperature fixation or staining artefacts. The average size and shape of synaptic vesicles, and AZM macromolecules and their relationships were similar regardless of which method was used [20,26]. However, as will be described below, staining by freeze-substitution makes apparent an assembly of macromolecules in the lumen of synaptic vesicles not evident after staining at room temperature. Detailed methods for tissue preparation, sectioning and collection of electron microscopy data have been described elsewhere; we used the software package EM3D (www.em3d.org) for reconstruction of volumetric datasets and generation of virtual slices, segmentation and rendering 3D surface models [17,20,21,26]. Of particular importance for our studies was the magnification at which the data were collected; higher magnification results in better 3D spatial resolution. We routinely used magnifications between $50\,000\times$ and $125\,000\times$.

The axon terminals in the cutaneous pectoris muscles were electrically activated using the following scheme [20]. After the muscles were pinned out in a Petri dish containing Ringer's solution, a 5 mm stretch of the cut end of its nerve was drawn into a suction electrode.

Simultaneously, the Ringer's solution was replaced with iso-osmotic Ringer's solution containing glutaraldhyde and the nerve was stimulated at 10 Hz; stimulation was terminated after 2 min when all neuromuscular junctions were fixed.

3. Layout of the active zone at frog neuromuscular junctions

As shown by 2D electron microscopy on tissue sections, each active zone in an axon terminal at frog neuromuscular junctions occupies a narrow band on the presynaptic membrane that can be 1 µm or more long (figure 1; see also [14,15,17]). The main body of the AZM extends throughout the length of the band. It is approximately 50 nm wide, projects up to approximately 75 nm from the presynaptic membrane at regular intervals, and rests in a shallow evagination in the presynaptic membrane, the active zone ridge. When examined in 3D using electron tomography, synaptic vesicles have three orthogonal diameters characteristic of an ellipsoid [26]. The three diameters vary from synaptic vesicle to synaptic vesicle, but the geometric mean of the diameters for each synaptic vesicle is similar, about 55 nm ($\pm 10\%$). Flanking each side of the main body of the AZM throughout its extent is a row of synaptic vesicles. In resting terminals, more than 98% of the synaptic vesicles flanking the AZM are docked; i.e. there is no detectable gap between or merging of the vesicle membrane and presynaptic membrane, as determined by electron tomography [26]. Conventional electron microscopy on freeze–fracture replicas of the interior of the presynaptic membrane reveals that, along each slope of the active zone ridge, the presynaptic membrane contains a double row of macromolecules that parallels the rows of docked synaptic vesicles [15,27]. The macromolecules are thought to include the active zone's Ca^{2+}-channels and Ca^{2+}-activated K^{+}-channels [28].

4. Organization of active zone material macromolecules and their linkage to docked synaptic vesicles

Electron tomography shows that the main body of the AZM is composed of a network of macromolecules that fall into several distinct classes (figure 1b,d; [17,20]). Ribs, spars and booms lie in different layers nearly parallel with the presynaptic membrane and nearly orthogonal to the median plane of the active zone: ribs are adjacent to the presynaptic membrane along the slopes of the active zone ridge, while spars are deep to the ribs and booms are deep to the spars. Each of these classes arises from a different core macromolecule serially arranged vertical to the presynaptic membrane near the midline of the AZM: ribs arise from beams, spars from steps, and booms from masts. Docked synaptic vesicles are typically connected to the ends of approximately four ribs, approximately two spars and approximately five booms. The connection sites formed by each class are on the synaptic vesicle hemisphere facing the AZM, and those of each class occupy a domain on the hemisphere according to the class's distance from the presynaptic membrane. Two pegs arranged in series along the length of each rib connect it to the presynaptic membrane. Another class of AZM macromolecules, pins, are outside
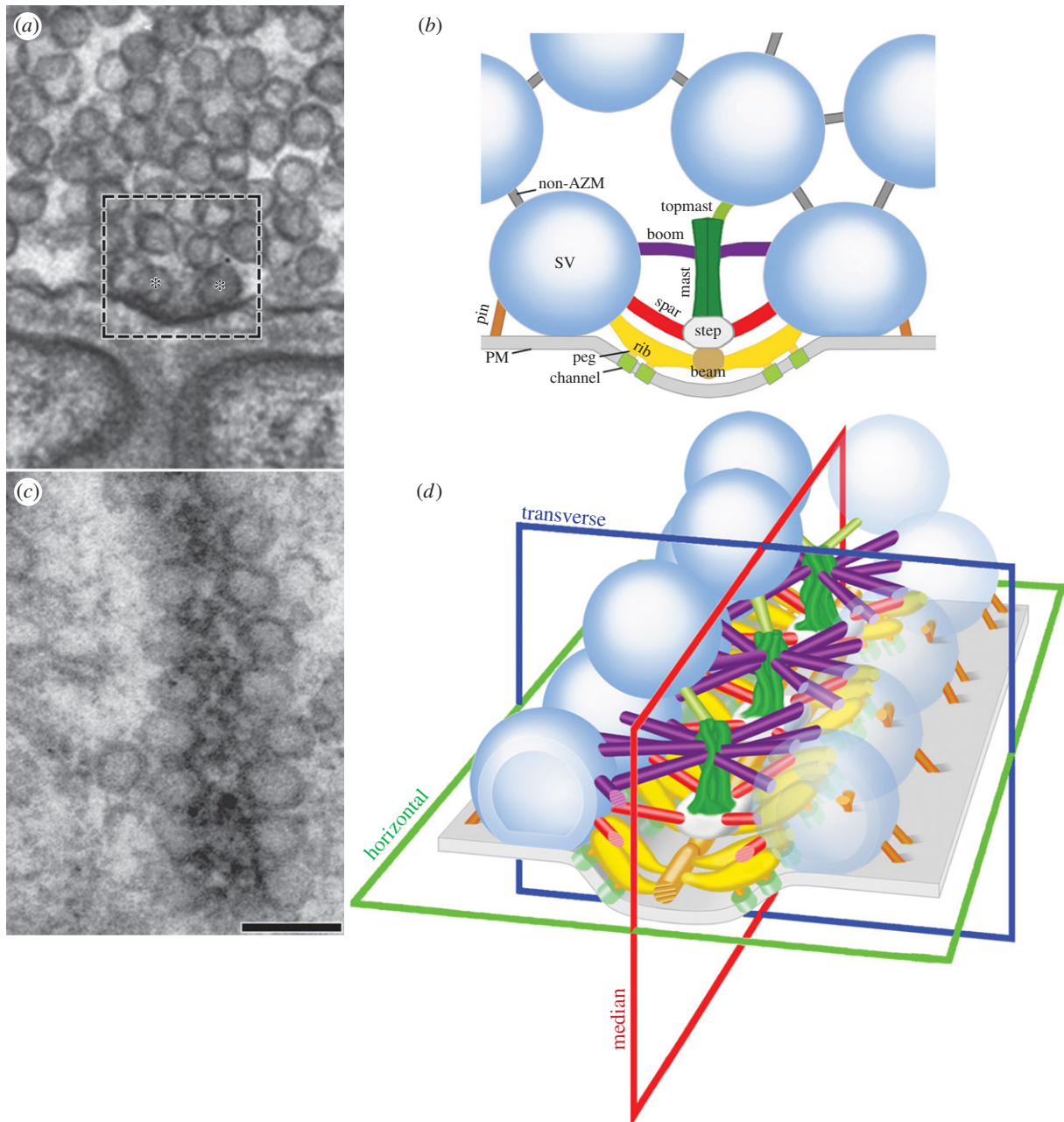
Figure 1. Arrangement of AZM at active zones on the presynaptic membrane of frog neuromuscular junctions. (*a*) A 2D electron micrograph from an approximately 80 nm thick tissue section cut in the transverse plane of an active zone. A dense aggregate of macromolecules, constituting the main body of AZM, is seated in the presynaptic membrane's active zone ridge and flanked by synaptic vesicles (asterisks) docked on the presynaptic membrane. The area in the box approximates the area shown in *b*. (*b*) Composite diagram of the relationships of AZM macromolecules exposed by electron tomography and viewed in the active zone's transverse plane. Ribs, spars and booms arise from beams, steps and masts in the main body of the AZM to connect to specific domains of the membrane of docked synaptic vesicles (SV) according to their depth/distance from the presynaptic membrane (PM). Pegs link ribs to macromolecules, thought to include Ca^{2+}-channels and Ca^{2+}-activated K^+-channels in the pre-synaptic membrane, while beyond the main body of AZM, the pins link the vesicle membrane directly to the presynaptic membrane. The topmast links the deep end of the mast to an undocked synaptic vesicle. Non-AZM macromolecules connect the membrane of docked synaptic vesicles to the membrane of nearby undocked synaptic vesicles and are similar to filamentous macromolecules that connect undocked synaptic vesicles to each other. (*c*) A 2D electron micrograph from an approximately 50 nm thick tissue section cut in the horizontal plane of an active zone. The main body of the AZM in this plane is a band. The docked synaptic vesicles are arranged in a single row on each side of it. Scale bar, 100 nm for *a* and *c*. (*d*) A 3D schematic of the active zone showing the same structures, with the same colour code, that are labelled in *b*, with indicators of the active zone's horizontal, transverse and median planes. (*a*) and (*c*) adapted from [20]; (*b*) and (*d*) from [21].

the main body of the AZM. Approximately, four pins directly link the synaptic vesicle hemisphere facing away from the main body of the AZM to the presynaptic membrane. The connection sites of pins and ribs on the vesicle membrane encircle the docked synaptic vesicle's fusion domain, i.e. the portion that contributes to the vesicle membrane–presynaptic membrane contact site. The dimensions of the different classes of AZM macromolecules and their distances from each other and the presynaptic membrane are given elsewhere [20], but

we note here the average distance of the rib–vesicle membrane and pin–vesicle membrane connection sites to the presynaptic membrane is only approximately 10 nm.

Each member of a class of AZM macromolecules appears large enough in diameter to accommodate several proteins, and, although some proteins may extend from one macro-molecule into another at their connection site, each class is considered functionally unique. The close proximity of the macromolecules has made it difficult to histochemically

localize proteins known from biochemistry to be involved in the docking of synaptic vesicles to specific classes of AZM macromolecules. We have discussed elsewhere [20,21,26] how certain proteins shown to be involved with docking might be distributed among the AZM macromolecules. Of particular interest here is the location of the vesicle membrane proteins synaptobrevin and synaptotagmin and the presynaptic membrane proteins syntaxin and SNAP-25. Cytosolic portions of synaptobrevin, syntaxin and SNAP-25 [29,30] interact to form a coiled-coil, the so-called SNARE core complex, which generates force [31] that overcomes the repulsive forces between the vesicle membrane and presynaptic membrane and brings the two membranes into contact during docking [2–4,32]. The cytosolic portion of synaptotagmin is the vesicle membrane's Ca^{2+}-sensor [33–37]. Spatial constraints and other considerations [20,26] make it seem likely that the SNARE core complex is a component of pins and the proximal segment of ribs, i.e. the rib segment between the vesicle membrane and the peg proximal to it, while synaptotagmin is also likely to be a component of the proximal segment of the ribs. The frequency and distribution of the peg–presynaptic membrane connection sites is similar to that of the macromolecules in the presynaptic membrane seen in freeze–fracture replicas [17,18], indicating that the pegs are connected to the presynaptic membrane macromolecules and that they probably include the cytosolic portions of the presynaptic membrane's Ca^{2+}-channels [38] and Ca^{2+}-activated K^+-channels.

5. Topmasts and non-active zone material macromolecules

Topmasts extend from the deep end of masts to connect to nearby undocked synaptic vesicles [20]. The linkage of undocked synaptic vesicles to the AZM may increase their probability of replacing docked synaptic vesicles after the latter fuse with and flatten into the presynaptic membrane to be retrieved beyond the active zone for recycling [25,39].

In addition to its connection to approximately 15 filamentous AZM macromolecules, a docked synaptic vesicle is connected to approximately 10 filamentous non-AZM macromolecules (figures 1b and 2; [20,21]), which link it to nearby undocked synaptic vesicles and other organelles. The non-AZM macromolecules connect to docked synaptic vesicles on the hemisphere facing away from the main body of the AZM [21]. They are similar in appearance to filamentous macromolecules that link undocked synaptic vesicles throughout axon terminals at frog neuromuscular junctions and at other synapses [40–45]. The disassembly and reassembly of such linkages must play a role in the regulation of synaptic vesicle trafficking [46]. However, to date, there is no evidence that they play a direct role in guiding undocked synaptic vesicles to docking sites on the presynaptic membrane [20].

6. Alignment and linkage of synaptic vesicle macromolecules to active zone material macromolecules

We observed that staining neuromuscular junctions with osmium tetroxide and uranyl acetate in acetone by freeze-substitution exposed an interconnected assembly of
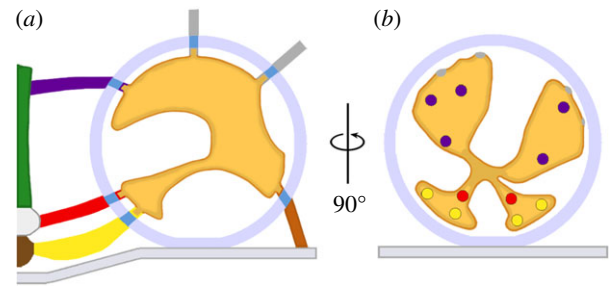
Figure 2. Linkage of macromolecules in docked synaptic vesicles to AZM macromolecules. (a) A schematic profile of a docked synaptic vesicle viewed in the transverse plane of the active zone. The interconnected assembly of macromolecules in the synaptic vesicle lumen is linked by its nubs to macromolecules that span the vesicle membrane and connect to AZM and non-AZM macromolecules. (b) The same docked synaptic vesicle rotated 90° and viewed from the main body of AZM in the median plane. The coloured spots on the radial arms of the luminal assembly mark regions connected by nubs and their membrane-spanning macromolecules to specific classes of AZM and non-AZM macromolecules.

macromolecules in the lumen of synaptic vesicles not evident after staining at room temperature [21]. The luminal assembly occupies approximately 10% of the lumen's volume, and it has a chiral bilateral shape that is similar from synaptic vesicle to synaptic vesicle. Characteristically, irregular arms radiate from near the lumen's centre to connect by nubs to the luminal surface of the vesicle membrane (figure 2). The number of nub connection sites on the vesicle membrane (approx. 25) is similar from synaptic vesicle to synaptic vesicle, and, at these sites, the nubs are linked to stained macromolecules that span the membrane. The nub connection sites on the luminal surface of the vesicle membrane are paired with, and linked by their transmembrane macromolecules to, AZM and non-AZM macromolecules at the connection sites of these macromolecules on the cytosolic surface of the vesicle membrane (figure 2). Thus, the synaptic vesicle proteins that interact with AZM macromolecules to mediate docking are not randomly distributed in the vesicle membrane but, rather, are situated in stereotypically arranged membrane macromolecules anchored by the luminal assembly.

For docked synaptic vesicles, the orientation of the luminal assembly's shape, with respect to the presynaptic membrane and the median plane of the active zone, is similar from synaptic vesicle to synaptic vesicle, whereas for undocked synaptic vesicles there is no common orientation (figure 3; [21]). Thus, in order for undocked synaptic vesicles to dock they must rotate so the shape of the luminal assembly is properly aligned with the presynaptic membrane and median plane of the active zone. This enables the appropriate vesicle membrane macromolecules anchored by the assembly to interact with the different classes of AZM macromolecules. The predetermined arrangement of macromolecules in the vesicle membrane of undocked synaptic vesicles that are destined to interact with the AZM macromolecules during docking indicates that the fusion domain of the vesicle membrane is also predetermined. This raises the issue of whether or not the fusion domain of the vesicle membrane is in some way specialized for fusion with the presynaptic membrane [21]. The linkage of the luminal assembly to specifically arranged macromolecules in the vesicle membrane during docking also raises the problem of determining the fate of the luminal assembly after the vesicle membrane of a
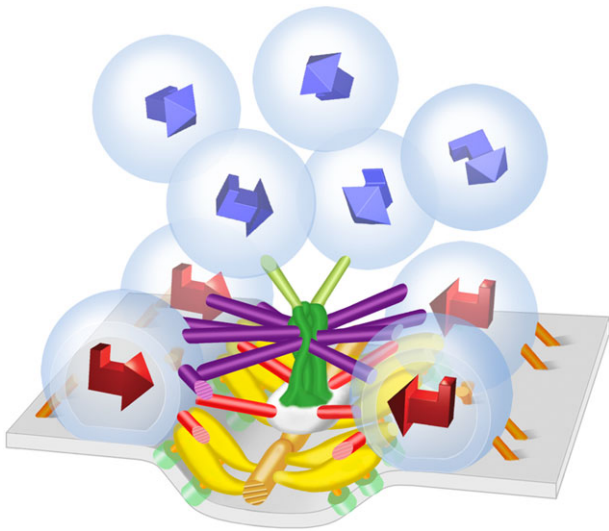
Figure 3. Rotation of undocked synaptic vesicles and alignment of synaptic vesicle macromolecules with AZM macromolecules during docking. The chiral shape of the luminal assembly of macromolecules is stereotypic for both docked and undocked synaptic vesicles. Represented by 3D arrows, the orientation of the shape of the luminal assemblies in docked synaptic vesicles (red arrows) is the same with respect to the presynaptic membrane and the midline of the main body of AZM. The orientation of the shape of the luminal assemblies in undocked synaptic vesicles (blue arrows) varies from vesicle to vesicle. Thus, undocked synaptic vesicles must rotate in order for the appropriate vesicle membrane-spanning macromolecules, anchored by the luminal assembly (figure 2), to align with and connect to AZM macromolecules. (From [21].)

docked synaptic vesicle fuses with and flattens into the presynaptic membrane to be then retrieved elsewhere and reformed into a fully functioning synaptic vesicle. Such recycling can occur in less than 1 min [47]. It may be that when docked synaptic vesicles fuse with the presynaptic membrane, the shape of the luminal assembly is temporarily altered to accommodate the flattening of the synaptic vesicle membrane into the presynaptic membrane, but the assembly still helps maintain the relative positioning of the membrane macromolecules so that the docking of recycled synaptic vesicles can occur in such a timely manner.

Biochemistry indicates that proteins in the lumen of synaptic vesicles are portions of ones that span the vesicle membrane, such as synaptobrevin and synaptotagmin [48]. However, based on their primary structure, synaptobrevin, synaptotagmin and nearly all other transmembrane vesicle membrane proteins could extend into the lumen for only a small fraction of their diameter [49–52]. On the other hand, the length of the luminal portion of the transmembrane protein SV2 is much greater than the diameter of the synaptic vesicle lumen [53]. Thus, folded luminal portions of SV2 are likely to serve as the luminal assembly's mainstay for the attachment of the luminal portions of the other transmembrane proteins.

7. Sequence of connections formed between undocked synaptic vesicles and active zone material macromolecules during docking

In order to observe the relationships between the different classes of AZM macromolecules and undocked synaptic

vesicles in the process of replacing former docked synaptic vesicles that had fused with the presynaptic membrane during synaptic activity, we glutaraldehyde-fixed axon terminals for electron tomography while electrically stimulating the axons [20]. In such preparations, there were numerous docking sites at which the former docked synaptic vesicles had fused with and flattened into the presynaptic membrane so the vesicle membrane was no longer distinguishable from the presynaptic membrane. In all such sites there were nearby undocked synaptic vesicles. Those undocked synaptic vesicles approximately 25–40 nm from their closest point on the presynaptic membrane were connected primarily to the booms, while those approximately 15–25 nm from the presynaptic membrane were connected primarily to booms and spars and those approximately 5–15 nm from the presynaptic membrane were connected to booms, spars, ribs and pins, in a manner similar to their connections to the different classes of AZM macromolecules when docked in resting axon terminals. These findings led to the conclusion that synaptic vesicle movement towards and maintenance at docking sites on the presynaptic membrane are directed by formation of an orderly succession of stable connections between the appropriate macromolecules in the vesicle membrane and the different classes of AZM macromolecules according to their distance from the presynaptic membrane (figure 4). Possible mechanisms for the movement of synaptic vesicles from booms to spars to ribs and pins are explained in [20] and [21].

After a docked synaptic vesicle fuses with the presynaptic membrane the proteins of the SNARE complex disassemble so that synaptobrevin in the vesicle membrane dissociates from the syntaxin and SNAP-25 of the presynaptic membrane [54]. Accordingly, if the SNARE proteins are components of the ribs and pins, as we suggest [20,26], a portion of the ribs and pins must disassemble from the AZM and remain with the vesicle membrane after it fuses with and flattens into the presynaptic membrane for recycling. Undocked synaptic vesicles would carry a portion of the ribs and pins to participate in complete rib and pin reassembly in the AZM as they become docked. We noted that the length of pins connecting undocked synaptic vesicles to the presynaptic membrane at vacated docking sites was in certain cases three to four times greater than the length of pins associated with docked synaptic vesicles [20] and that the pin length was directly proportional to the undocked synaptic vesicles' distance from the presynaptic membrane (figure 4). Accordingly, during synaptic vesicle docking, the pins, if not all AZM macromolecules that connect to the synaptic vesicles, undergo significant structural modification.

8. Priming and the positioning of Ca^{2+}-channels

At typical synapses, a small proportion of docked synaptic vesicles fuse with the presynaptic membrane after the arrival of a nerve impulse. This has led to the concept that the fraction of docked synaptic vesicles that undergo fusion become primed by transitioning from fusion-incompetent to fusion-competent [3,55–58]. It is generally accepted that for the vesicle membrane and presynaptic membrane to fuse they must be energetically destabilized at their contact site, and, with sufficient destabilization, the lipid bilayers spontaneously undergo a series of rearrangements to form a
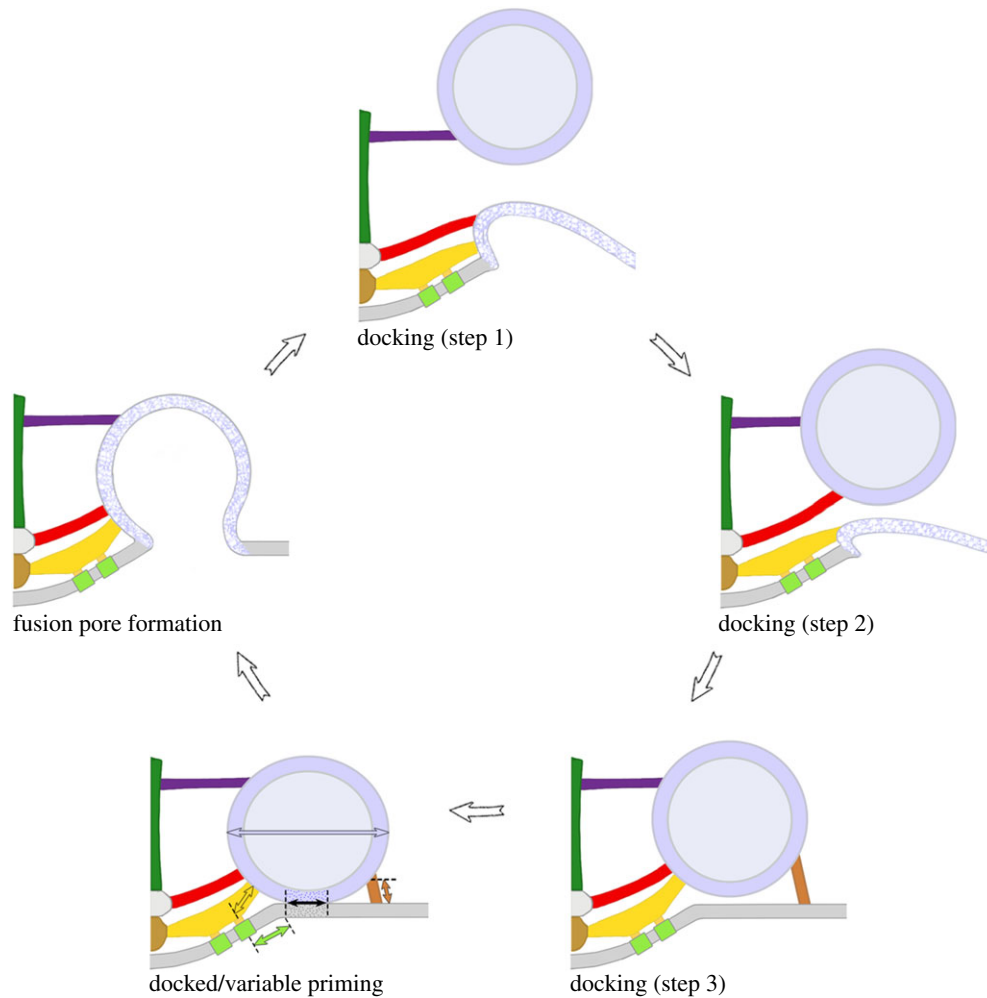
Figure 4. Model for AZM-mediated docking, priming and Ca^{2+}-triggered vesicle membrane–presynaptic membrane fusion. After a docked synaptic vesicle fuses with and flattens into the presynaptic membrane (blue and white stippled membrane), an undocked synaptic vesicle is directed towards and held in contact with the vacated docking site on the presynaptic membrane by a stepwise progression of stable interactions between it and multiple booms, spars and ribs of the AZM (colour-coded as in figure 1b). Once a synaptic vesicle is docked it undergoes variable priming: the pins and proximal rib segments that link it to the presynaptic membrane shorten and lengthen in dynamic equilibrium (copper and gold double-headed arrows), generating variable force that brings about coordinated variation in (1) the extent of the vesicle membrane–presynaptic membrane contact area and the stability of the lipid bilayers at the contact site (double-headed black arrow), in (2) the proximity of proximal pegs and their associated calcium channels (double-headed green arrow) to the vesicle membrane's Ca^{2+}-sensors and in (3) the synaptic vesicle's eccentricity (blue double-headed arrow) in the plane of the presynaptic membrane. Accordingly, docked synaptic vesicles are most primed when their pins and proximal rib segments are shortest, their vesicle membrane–presynaptic membrane contact areas are largest, their lipid bilayers are most destabilized towards fusion threshold, their associated Ca^{2+}-channels are, on average, in closest proximity to it and they are most eccentric in shape. The membrane of docked synaptic vesicles that are most primed at the moment a nerve impulse arrives has the greatest probability of merging with the presynaptic membrane to form a fusion pore. Fusion occurs while the synaptic vesicle is still attached to the AZM macromolecules. Figure adapted from [20] and [26].

shared fusion pore [1], but see [59–61]. Thus, it is reasonable to expect that priming of docked synaptic vesicles for fusion with the presynaptic membrane involves the application of force to the vesicle membrane–presynaptic membrane contact site, which provides the energy to drive the local destabilization of the membranes towards fusion threshold. Such force might be generated, at least in part, by a regulated tightening of the coiled SNARE core complex [2] similar to that which brings the vesicle membrane into contact with the presynaptic membrane during docking. Moreover, any decrease in the distance of Ca^{2+}-channels from the vesicle membrane–presynaptic membrane contact site that occurs after docking would be expected to increase the probability that Ca^{2+} entering the cytosol through the channels will reach the vesicle membrane's Ca^{2+}-sensors, synaptotagmin, to trigger the events that ultimately overcome the vesicle membrane–presynaptic membrane fusion threshold [37,58]; a decrease

in distance between the Ca^{2+}-channels and Ca^{2+}-sensors by as little as 5 nm may have a profound effect on synaptic vesicle fusion probability [62]. These mechanisms for priming, coupled with the concept of a docked synaptic vesicle switching from an unprimed to a primed state, have been directly or indirectly suggested from biochemical and electrophysiological studies [3,55–58,63].

We searched for the structural correlates of priming among docked synaptic vesicles at frog neuromuscular junctions. We found in resting terminals that the extent of the vesicle membrane–presynaptic membrane contact area from docked synaptic vesicle to docked synaptic vesicle varies by more than an order of magnitude (from 50 to $650\,nm^2$) with a normal frequency distribution [26]. In muscles fixed during repetitive nerve stimulation, the frequency distribution of the vesicle membrane–presynaptic membrane contact areas was shifted to the left while from muscles fixed 1 h after such

stimulation the frequency distribution was fully recovered. Thus, docked synaptic vesicles with relatively large contact areas preferentially fuse with the presynaptic membrane during evoked synaptic activity and the frequency distribution of contact areas is dynamic and in equilibrium at rest. Positively correlated with the extent of a docked synaptic vesicle's contact area at rest, is the extent of the synaptic vesicle's overall ellipsoid shape, the long diameter running parallel to the presynaptic membrane and orthogonal to the main body of the AZM, indicating that variable force is being applied to docked synaptic vesicles towards the presynaptic membrane and the midline of the AZM. To examine the origin of this force, we measured the length of the pins and proximal segments of ribs per synaptic vesicle (figure 4), which link the vesicle membrane of each docked synaptic vesicle to the presynaptic membrane near the contact site, and found that the average length of each class of AZM component is negatively correlated with the extent of a docked synaptic vesicle's contact area, as is the average displacement of the rib's proximal peg and the associated presynaptic membrane macromolecule towards the vesicle membrane–presynaptic membrane contact site.

Taken together, our findings lead to a hypothesis for the priming of docked synaptic vesicles at frog neuromuscular junctions based on continually variable AZM-mediated forces (figure 4; fully discussed in [26]). Accordingly, after a synaptic vesicle docks, as a result of its vesicle membrane forming connections to multiple pins and ribs [20], each of the pins and proximal rib segments independently shortens and lengthens in dynamic equilibrium, while vesicle membrane–presynaptic membrane contact is maintained. The shortening of the pins and the proximal rib segments applies force to the docked synaptic vesicle, which increases the eccentricity of its overall shape, and to the vesicle membrane–presynaptic membrane contact site, which brings about an increase in the vesicle membrane–presynaptic membrane contact area, delivering energy that drives the local destabilization of the membranes' bilayers towards the fusion threshold. Force provided by shortening of the proximal segments of the ribs also brings about the selective displacement of proximal pegs and their associated presynaptic membrane macromolecules, which include Ca^{2+}-channels, towards the vesicle membrane–presynaptic membrane contact site and the nearby synaptotagmin. This would increase the probability of the Ca^{2+} that enters the cytosol through the channels reaching synaptotagmin at a concentration necessary to trigger the events that ultimately overcome the vesicle membrane–presynaptic membrane fusion threshold [37,58]. Moreover, Ca^{2+} influx through these channels might be enhanced by increased mechanical force on them, as has been shown for voltage-dependent K^+-channels [64]. Thus, according to our hypothesis, the priming of a docked synaptic vesicle for fusion with the presynaptic membrane is not a binary transition from an unprimed state to a primed state, as suggested by others [3,55–58]. Rather, it is an energetic manifestation of continually varying AZM-mediated forces exerted on the vesicle membrane–presynaptic membrane contact site and its associated Ca^{2+}-channels. The SNARE core complex is thought to tighten (shorten) and loosen (lengthen) in dynamic equilibrium and, thus, if it is a component of proximal rib segments and pins, as we suggest, it may well provide the priming force. As an extension of our hypothesis, the relatively few docked synaptic vesicles at resting frog neuromuscular junctions that fuse with the presynaptic membrane when a nerve impulse arrives [24,65] are mostly, if not entirely, among those primed to the greatest extent at that moment. Moreover, because the membranes at the vesicle membrane–presynaptic membrane contact sites having large contact areas would be more energetically destabilized and, therefore, closer to fusion threshold than those of other vesicle membrane–presynaptic membrane contact sites, they may also have a higher probability of spontaneously fusing as a result of, for example, thermal fluctuations in the membranes. This might account for most, if not all, of the spontaneous vesicle membrane–presynaptic membrane fusions detected by electrophysiology as miniature endplate potentials at resting neuromuscular junctions [66].

9. Comment

The proteins directly involved in the docking of synaptic vesicles and the Ca^{2+}-triggered fusion of docked synaptic vesicles with the presynaptic membrane are thought to be similar for all synapses. At all synapses in vertebrate and in invertebrate nervous systems where AZM relationships have been examined by electron tomography, the AZM links synaptic vesicle membranes to the presynaptic membrane [17,19,44,45,63,67–71]. Although it is not known whether AZM macromolecules are connected to PM macromolecules thought to include Ca^{2+}-channels at neuron-to-neuron synapses, as at frog and mouse neuromuscular junctions [17,19], conventional electron microscopy has shown that the AZM is very near such macromolecules [72,73]. Thus, our findings on the structure of the active zone at frog neuromuscular junctions make it likely that the SNARE core complex, synaptotagmin, and the cytosolic portions of Ca^{2+}-channels are common constituents of AZM at all types of synapses even if there are differences in the number, size, and shape of AZM patches and in the positioning of their associated docked synaptic vesicles [9]. Such gross differences together with any differences in the organization and relationships of AZM macromolecules accompanying them may subserve synapse-specific requirements for effective chemical transmission of nerve impulses from the presynaptic to postsynaptic cell [19]. For example, the structural organization of the AZM may influence the number of synaptic vesicles that can dock at an active zone, the rate and efficiency of docking and priming, and the Ca^{2+}-triggering of synaptic vesicle fusion with the presynaptic membrane during synaptic activity. The methods we have used for characterizing the role of AZM in the function of active zones at frog neuromuscular junctions can be used for the same purpose at any synapse.

References

1. Chernomordik LV, Kozlov MM. 2008 Mechanics of membrane fusion. *Nat. Struct. Mol. Biol.* **15**, 675–683. (doi:10.1038/nsmb.1455)

2. Jahn R, Fasshauer D. 2012 Molecular machines governing exocytosis of synaptic vesicles. *Nature* **490**, 201–207. (doi:10.1038/nature11320)

3. Rizo J, Rosenmund C. 2008 Synaptic vesicle fusion. *Nat. Struct. Mol. Biol.* **15**, 665–674. (doi:10.1038/nsmb.1450)

4. Südhof TC, Rothman JE. 2009 Membrane fusion: grappling with SNARE and SM proteins. *Science* **323**, 474–477. (doi:10.1126/science.1161748)

5. Gray EG, Pease HL. 1971 On understanding the organisation of the retinal receptor synapses. *Brain Res.* **35**, 1–15. (doi:10.1016/0006-8993(71)90591-9)

6. Raviola E, Gilula NB. 1975 Intramembrane organization of specialized contacts in the outer plexiform layer of the retina. A freeze-fracture study in monkeys and rabbits. *J. Cell Biol.* **65**, 192–222. (doi:10.1083/jcb.65.1.192)

7. Shaw SR, Meinertzhagen IA. 1986 Evolutionary progression at synaptic connections made by identified homologous neurones. *Proc. Natl Acad. Sci. USA* **83**, 7961–7965. (doi:10.1073/pnas.83.20.7961)

8. Koenig JH, Ikeda K. 1999 Contribution of active zone subpopulation of vesicles to evoked and spontaneous release. *J. Neurophysiol.* **81**, 1495–1505.

9. Zhai RG, Bellen HJ. 2004 The architecture of the active zone in the presynaptic nerve terminal. *Physiology* (Bethesda) **19**, 262–270. (doi:10.1152/physiol.00014.2004)

10. Palade GE. 1954 Electron microscope observations of interneuronal and neuromuscular synapses. *Anat. Rec.* **118**, 335.

11. Palay SL. 1954 Electron microscope study of the cytoplasm of neurons. *Anat. Rec.* **118**, 336.

12. Palay SL. 1956 Synapses in the central nervous system. *J. Biophys. Biochem. Cytol.* **2**, 193–202. (doi:10.1083/jcb.2.4.193)

13. Gray EG. 1963 Electron microscopy of presynaptic organelles of the spinal cord. *J. Anat.* **97**, 101–106.

14. Couteaux R, Pecot-Dechavassine M. 1970 Synaptic vesicles and pouches at the level of 'active zones' of the neuromuscular junction. *C. R. Hebd. Seances Acad. Sci. D* **271**, 2346–2349.

15. Heuser JE, Reese TS, Landis DM. 1974 Functional changes in frog neuromuscular junctions studied with freeze-fracture. *J. Neurocytol.* **3**, 109–131. (doi:10.1007/BF01111936)

16. Ress D, Harlow ML, Schwarz M, Marshall RM, McMahan UJ. 1999 Automatic acquisition of fiducial markers and alignment of images in tilt series for electron tomography. *J. Electron Microsc. (Tokyo)* **48**, 277–287. (doi:10.1093/oxfordjournals.jmicro.a023679)

17. Harlow ML, Ress D, Stoschek A, Marshall RM, McMahan UJ. 2001 The architecture of active zone material at the frog's neuromuscular junction. *Nature* **409**, 479–484. (doi:10.1038/35054000)

18. Ress DB, Harlow ML, Marshall RM, McMahan UJ. 2004 Methods for generating high-resolution structural models from electron microscope tomography data. *Structure* **12**, 1763–1774. (doi:10.1016/j.str.2004.07.022)

19. Nagwaney S, Harlow ML, Jung JH, Szule JA, Ress D, Xu J, Marshall RM, McMahan UJ. 2009 Macromolecular connections of active zone material to docked synaptic vesicles and presynaptic membrane at neuromuscular junctions of mouse. *J. Comp. Neurol.* **513**, 457–468. (doi:10.1002/cne.21975)

20. Szule JA, Harlow ML, Jung JH, De-Miguel FF, Marshall RM, McMahan UJ. 2012 Regulation of synaptic vesicle docking by different classes of macromolecules in active zone material. *PLoS ONE* **7**, e33333. (doi:10.1371/journal.pone.0033333)

21. Harlow ML, Szule JA, Xu J, Jung JH, Marshall RM, McMahan UJ. 2013 Alignment of synaptic vesicle macromolecules with the macromolecules in active zone material that direct vesicle docking. *PLoS ONE* **8**, e69410. (doi:10.1371/journal.pone.0069410)

22. Frank J. 2006 *Electron tomography : methods for three-dimensional visualization of structures in the cell*, 2nd edn. New York, NY: Springer.

23. McDonald K, Muller-Reichert T. 2002 Cryomethods for thin section electron microscopy. *Methods Enzymol.* **351**, 96–123. (doi:10.1016/S0076-6879(02)51843-7)

24. Heuser JE, Reese TS, Dennis MJ, Jan Y, Jan L, Evans L. 1979 Synaptic vesicle exocytosis captured by quick freezing and correlated with quantal transmitter release. *J. Cell Biol.* **81**, 275–300. (doi:10.1083/jcb.81.2.275)

25. Heuser JE, Reese TS. 1981 Structural changes after transmitter release at the frog neuromuscular junction. *J. Cell Biol.* **88**, 564–580. (doi:10.1083/jcb.88.3.564)

26. Jung JH, Szule JA, Marshall RM, McMahan UJ. 2015 Variable priming of a docked synaptic vesicle. (Submitted).

27. Pumplin DW, Reese TS, Llinas R. 1981 Are the presynaptic membrane particles the calcium channels? *Proc. Natl Acad. Sci. USA* **78**, 7210–7213. (doi:10.1073/pnas.78.11.7210)

28. Robitaille R, Garcia ML, Kaczorowski GJ, Chariton MP. 1993 Functional colocalization of calcium and calcium-gated potassium channels in control of transmitter release. *Neuron* **11**, 645–655. (doi:10.1016/0896-6273(93)90076-4)

29. Weber T, Zemelman BV, McNew JA, Westermann B, Gmachl M, Parlati F, Söllner TH, Rothman JE. 1998 SNAREpins: minimal machinery for membrane fusion. *Cell* **92**, 759–772. (doi:10.1016/S0092-8674(00)81404-X)

30. Hammarlund M, Palfreyman MT, Watanabe S, Olsen S, Jorgensen EM. 2007 Open syntaxin docks synaptic vesicles. *PLoS Biol.* **5**, e198. (doi:10.1371/journal.pbio.0050198)

31. Min D, Kim K, Hyeon C, Hoon Cho Y, Shin Y-K, Yoon T-Y. 2013 Mechanical unzipping and rezipping of a single SNARE complex reveals hysteresis as a force-generating mechanism. *Nat. Commun.* **4**, 1705. (doi:10.1038/ncomms2692)

32. Sudhof TC. 2013 Neurotransmitter release: the last millisecond in the life of a synaptic vesicle. *Neuron* **80**, 675–690. (doi:10.1016/j.neuron.2013.10.022)

33. Brose N, Petrenko A, Sudhof T, Jahn R. 1992 Synaptotagmin: a calcium sensor on the synaptic vesicle surface. *Science* **256**, 1021–1025. (doi:10.1126/science.1589771)

34. Geppert M, Goda Y, Hammer RE, Li C, Rosahl TW, Stevens CF, Südhof TC. 1994 Synaptotagmin I: a major Ca^{2+} sensor for transmitter release at a central synapse. *Cell* **79**, 717–727. (doi:10.1016/0092-8674(94)90556-8)

35. Mackler JM, Drummond JA, Loewen CA, Robinson IM, Reist NE. 2002 The C_2B Ca^{2+}-binding motif of synaptotagmin is required for synaptic transmission *in vivo*. *Nature* **418**, 340–344. (doi:10.1038/nature00846)

36. Paddock BE, Striegel AR, Hui E, Chapman ER, Reist NE. 2008 Ca^{2+}-dependent, phospholipid-binding residues of synaptotagmin are critical for excitation–secretion coupling *in vivo*. *J. Neurosci.* **28**, 7458–7466. (doi:10.1523/JNEUROSCI.0197-08.2008)

37. Striegel AR, Biela LM, Evans CS, Wang Z, Delehoy JB, Sutton RB, Chapman ER, Reist NE. 2012 Calcium binding by synaptotagmin's C_2A domain is an essential element of the electrostatic switch that triggers synchronous synaptic transmission. *J. Neurosci.* **32**, 1253–1260. (doi:10.1523/JNEUROSCI.4652-11.2012)

38. Wong FK, Li Q, Stanley EF. 2013 Synaptic vesicle capture by CaV2.2 calcium channels. *Front. Cell Neurosci.* **7**, 101. (doi:10.3389/fncel.2013.00101)

39. Miller TM, Heuser JE. 1984 Endocytosis of synaptic vesicle membrane at the frog neuromuscular junction. *J. Cell Biol.* **98**, 685–698. (doi:10.1083/jcb.98.2.685)

40. Landis DM, Hall AK, Weinstein LA, Reese TS. 1988 The organization of cytoplasm at the presynaptic active zone of a central nervous system synapse. *Neuron* **1**, 201–209. (doi:10.1016/0896-6273(88)90140-7)

41. Hirokawa N, Sobue K, Kanda K, Harada A, Yorifuji H. 1989 The cytoskeletal architecture of the presynaptic terminal and molecular structure of synapsin 1. *J. Cell Biol.* **108**, 111–126. (doi:10.1083/jcb.108.1.111)

42. Gustafsson JS, Birinyi A, Crum J, Ellisman M, Brodin L, Shupliakov O. 2002 Ultrastructural organization of lamprey reticulospinal synapses in three dimensions. *J. Comp. Neurol.* **450**, 167–182. (doi:10.1002/cne.10310)

43. Siksou L *et al.* 2007 Three-dimensional architecture of presynaptic terminal cytomatrix. *J. Neurosci.* **27**, 6868–6877. (doi:10.1523/JNEUROSCI.1773-07.2007)

44. Fernandez-Busnadiego R, Zuber B, Maurer UE, Cyrklaff M, Baumeister W, Lucic V. 2010 Quantitative

analysis of the native presynaptic cytomatrix by cryoelectron tomography. *J. Cell Biol.* **188**, 145–156. (doi:10.1083/jcb.200908082)

45. Stigloher C, Zhan H, Zhen M, Richmond J, Bessereau J-L. 2011 The presynaptic dense projection of the *Caenorhabditis elegans* cholinergic neuromuscular junction localizes synaptic vesicles at the active zone through SYD-2/liprin and UNC-10/RIM-dependent interactions. *J. Neurosci.* **31**, 4388–4396. (doi:10.1523/JNEUROSCI.6164-10.2011)

46. Gabriel T, Garcia-Perez E, Mahfooz K, Goni J, Martinez-Turrillas R, Perez-Otano I, Lo DC, Wesseling JF. 2011 A new kinetic framework for synaptic vesicle trafficking tested in synapsin knock-outs. *J. Neurosci.* **31**, 11 563–11 577. (doi:10.1523/JNEUROSCI.1447-11.2011)

47. Betz WJ, Bewick GS. 1992 Optical analysis of synaptic vesicle recycling at the frog neuromuscular junction. *Science* **255**, 200–203. (doi:10.1126/science.1553547)

48. Takamori S *et al*. 2006 Molecular anatomy of a trafficking organelle. *Cell* **127**, 831–846. (doi:10.1016/j.cell.2006.10.030)

49. Trimble WS, Cowan DM, Scheller RH. 1988 VAMP-1: a synaptic vesicle-associated integral membrane protein. *Proc. Natl Acad. Sci. USA* **85**, 4538–4542. (doi:10.1073/pnas.85.12.4538)

50. Sudhof TC, Baumert M, Perin MS, Jahn R. 1989 A synaptic vesicle membrane protein is conserved from mammals to *Drosophila*. *Neuron* **2**, 1475–1481. (doi:10.1016/0896-6273(89)90193-1)

51. Perin MS, Johnston PA, Ozcelik T, Jahn R, Francke U, Südhof TC. 1991 Structural and functional conservation of synaptotagmin (p65) in Drosophila and humans. *J. Biol. Chem.* **266**, 615–622.

52. Sudhof TC, Lottspeich F, Greengard P, Mehl E, Jahn R. 1987 A synaptic vesicle protein with a novel cytoplasmic domain and four transmembrane regions. *Science* **238**, 1142–1144. (doi:10.1126/science.3120313)

53. Bajjalieh SM, Frantz GD, Weimann JM, McConnell SK, Scheller RH. 1994 Differential expression of synaptic vesicle protein 2 (SV2) isoforms. *J. Neurosci.* **14**, 5223–5235.

54. May AP, Whiteheart SW, Weis WI. 2001 Unraveling the mechanism of the vesicle transport ATPase NSF, the *N*-ethylmaleimide-sensitive factor. *J. Biol. Chem.* **276**, 21 991–21 994. (doi:10.1074/jbc.R100013200)

55. Klenchin VA, Martin TF. 2000 Priming in exocytosis: attaining fusion-competence after vesicle docking. *Biochimie* **82**, 399–407. (doi:10.1016/S0300-9084(00)00208-X)

56. Ma C, Li W, Xu Y, Rizo J. 2011 Munc13 mediates the transition from the closed syntaxin–Munc18 complex to the SNARE complex. *Nat. Struct. Mol. Biol.* **18**, 542–549. (doi:10.1038/nsmb.2047)

57. Martin TF. 2012 Role of PI(4,5)P$_2$ in vesicle exocytosis and membrane fusion. *Subcell Biochem.* **59**, 111–130. (doi:10.1007/978-94-007-3015-1_4)

58. Neher E, Sakaba T. 2008 Multiple roles of calcium ions in the regulation of neurotransmitter release. *Neuron* **59**, 861–872. (doi:10.1016/j.neuron.2008.08.019)

59. Han X, Wang C-T, Bai J, Chapman ER, Jackson MB. 2004 Transmembrane segments of syntaxin line the fusion pore of Ca^{2+}-triggered exocytosis. *Science* **304**, 289–292. (doi:10.1126/science.1095801)

60. Jackson MB, Chapman ER. 2008 The fusion pores of Ca^{2+}-triggered exocytosis. *Nat. Struct. Mol. Biol.* **15**, 684–689. (doi:10.1038/nsmb.1449)

61. Szule JA, Coorssen JR. 2004 Comment on 'Transmembrane segments of syntaxin line the fusion pore of Ca^{2+}-triggered exocytosis'. *Science* **306**, 813; author reply 813. (doi:10.1126/science.1101572)

62. Shahrezaei V, Delaney KR. 2004 Consequences of molecular-level Ca^{2+} channel and synaptic vesicle colocalization for the Ca^{2+} microdomain and neurotransmitter exocytosis: a Monte Carlo study. *Biophys. J.* **87**, 2352–2364. (doi:10.1529/biophysj.104.043380)

63. Imig C, Min S-W, Krinner S, Arancillo M, Rosenmund C, Südhof TC, Rhee J, Brose N, Cooper BH. 2014 The morphological and molecular nature of synaptic vesicle priming at presynaptic active zones. *Neuron* **84**, 416–431. (doi:10.1016/j.neuron.2014.10.009)

64. Schmidt D, del Marmol J, MacKinnon R. 2012 Mechanistic basis for low threshold mechanosensitivity in voltage-dependent K^+ channels. *Proc. Natl Acad. Sci. USA* **109**, 10 352–10 357. (doi:10.1073/pnas.1204700109)

65. Katz B, Miledi R. 1979 Estimates of quantal content during 'chemical potentiation' of transmitter release. *Proc. R. Soc. Lond. B* **205**, 369–378. (doi:10.1098/rspb.1979.0070)

66. Katz B. 1969 *The release of neural transmitter substances*. The Sherrington lectures, 10. Springfield, IL: Thomas.

67. Fernandez-Busnadiego R *et al*. 2013 Cryo-electron tomography reveals a critical role of RIM1α in synaptic vesicle tethering. *J. Cell Biol.* **201**, 725–740. (doi:10.1083/jcb.201206063)

68. Jiao W, Masich S, Franzén O, Shupliakov O. 2010 Two pools of vesicles associated with the presynaptic cytosolic projection in *Drosophila* neuromuscular junctions. *J. Struct. Biol.* **172**, 389–394. (doi:10.1016/j.jsb.2010.07.007)

69. Rostaing P *et al*. 2006 Analysis of synaptic ultrastructure without fixative using high-pressure freezing and tomography. *Eur. J. Neurosci.* **24**, 3463–3474. (doi:10.1111/j.1460-9568.2006.05234.x)

70. Siksou L, Triller A, Marty S. 2011 Ultrastructural organization of presynaptic terminals. *Curr. Opin. Neurobiol.* **21**, 261–268. (doi:10.1016/j.conb.2010.12.003)

71. Zampighi GA, Fain N, Zampighi LM, Cantele F, Lanzavecchia S, Wright EM. 2008 Conical electron tomography of a chemical synapse: polyhedral cages dock vesicles to the active zone. *J. Neurosci.* **28**, 4151–4160. (doi:10.1523/JNEUROSCI.4639-07.2008)

72. Dickinson-Nelson A, Reese TS. 1983 Structural changes during transmitter release at synapses in the frog sympathetic ganglion. *J. Neurosci.* **3**, 42–52.

73. Indriati DW, Kamasawa N, Matsui K, Meredith AL, Watanabe M, Shigemoto R. 2013 Quantitative localization of Cav2.1 (P/Q-type) voltage-dependent calcium channels in Purkinje cells: somatodendritic gradient and distinct somatic coclustering with calcium-activated potassium channels. *J. Neurosci.* **33**, 3668–3678. (doi:10.1523/JNEUROSCI.2921-12.2013)